Coyote Copper Mines Inc.
Copper Spring Project

Geogenius Exploration Consulting
Au-Ag-Cu deposits professional
Understanding an ore deposit is the only way to reveals its true value.

Jocelyn Pelletier, P.geo, Msc, F-SEG

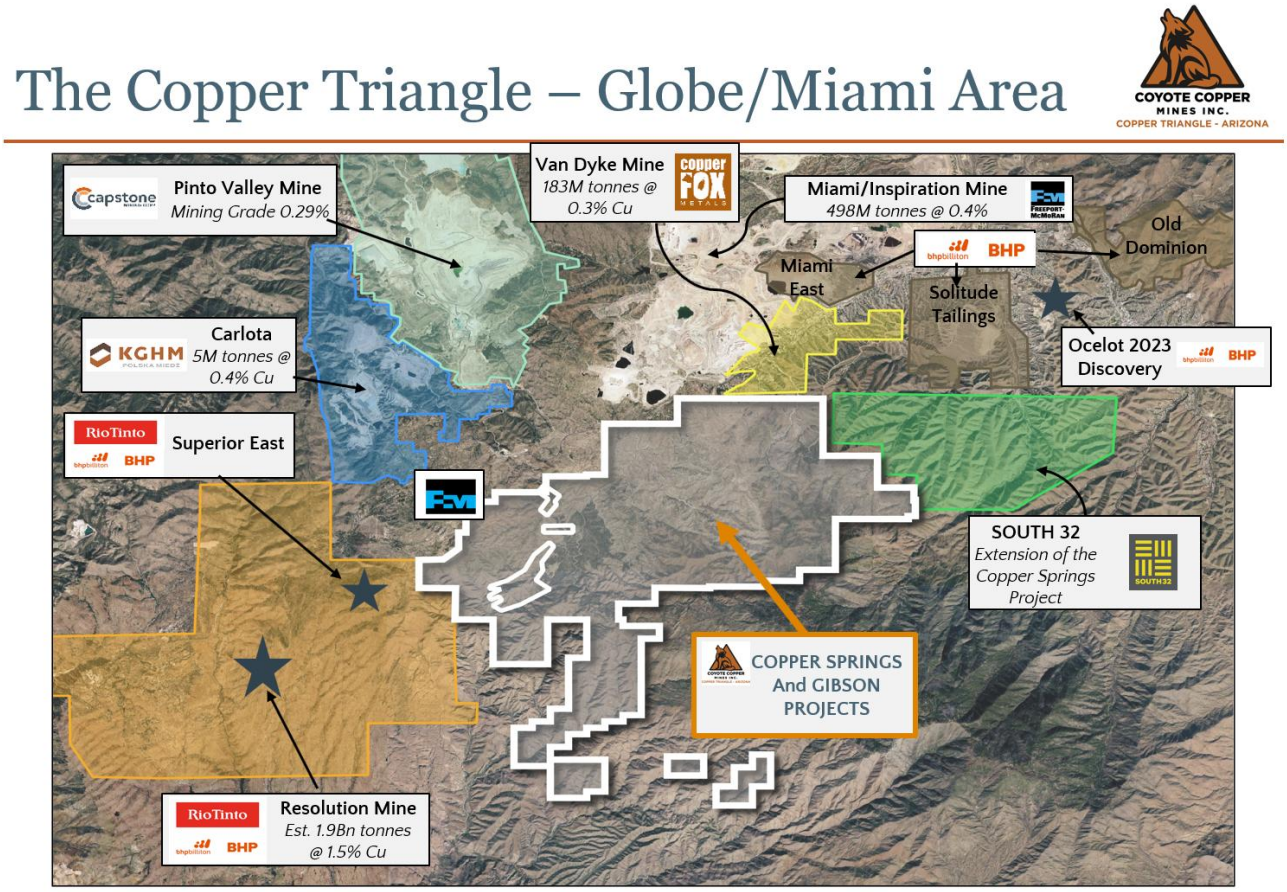
Preliminary Metallogeny Report

Evidence for Apical Position within a Porphyry Cu–Mo Deposit at Coyote Copper

Introduction

For years, geologists visiting the Copper Spring project interpreted the western outcrops as peripheral expressions of a Porphyry Copper Deposit (PCD), causing the property to lose appeal as a potential low-hanging-fruit target despite its proximity to major neighboring copper producers. However, a recent re-evaluation of the central and eastern portions of the project by Jocelyn Pelletier, principal consultant for Geogenius Exploration and MineOro Exploration, revealed a completely new geological interpretation, including evidence for at least three distinct intrusive apophyses belonging to a larger PCD system on the property.

Area Map



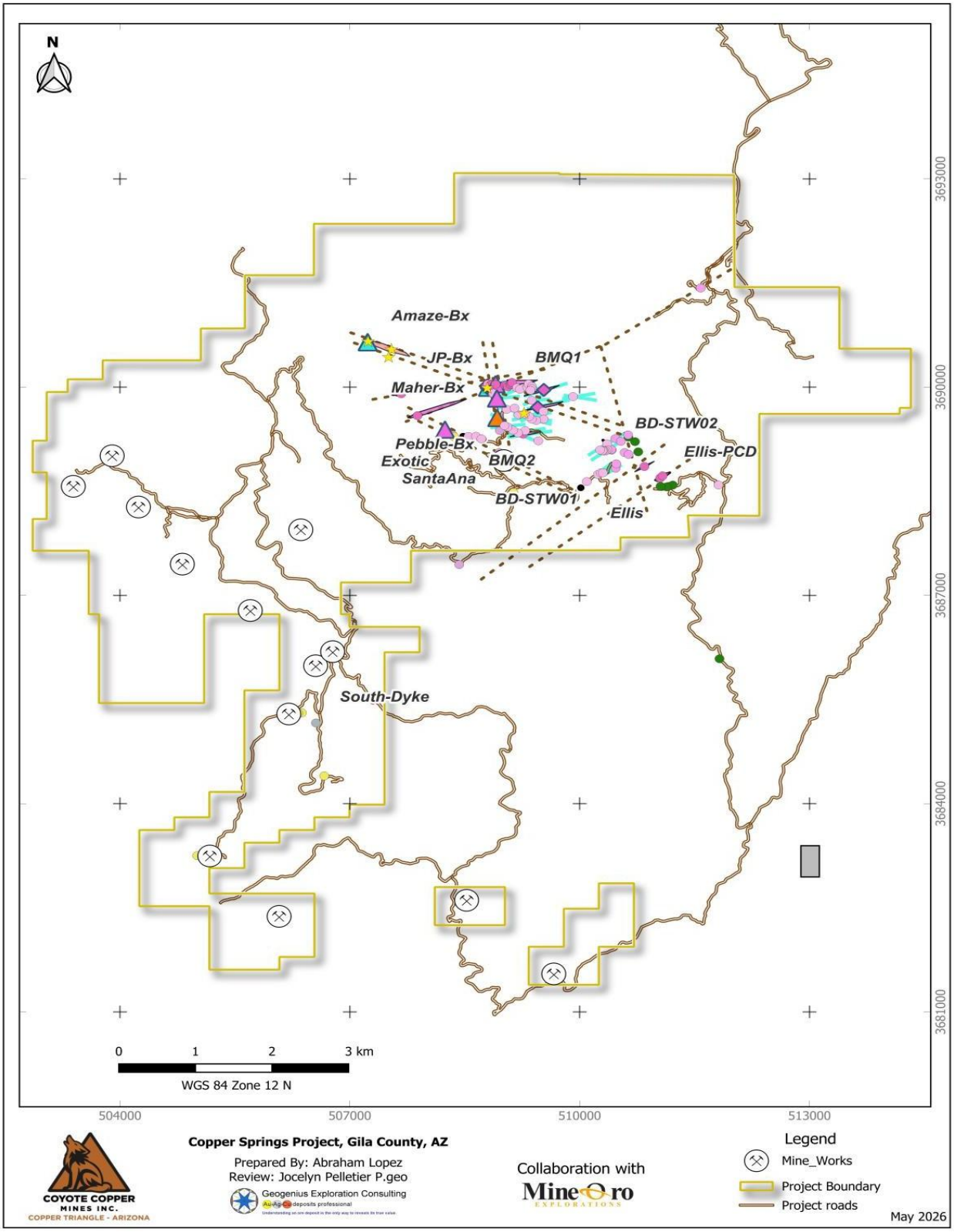


Figure 33: Schematic view of recent work performed in spring 2026 on the Copper Spring Project. (1:80,000)

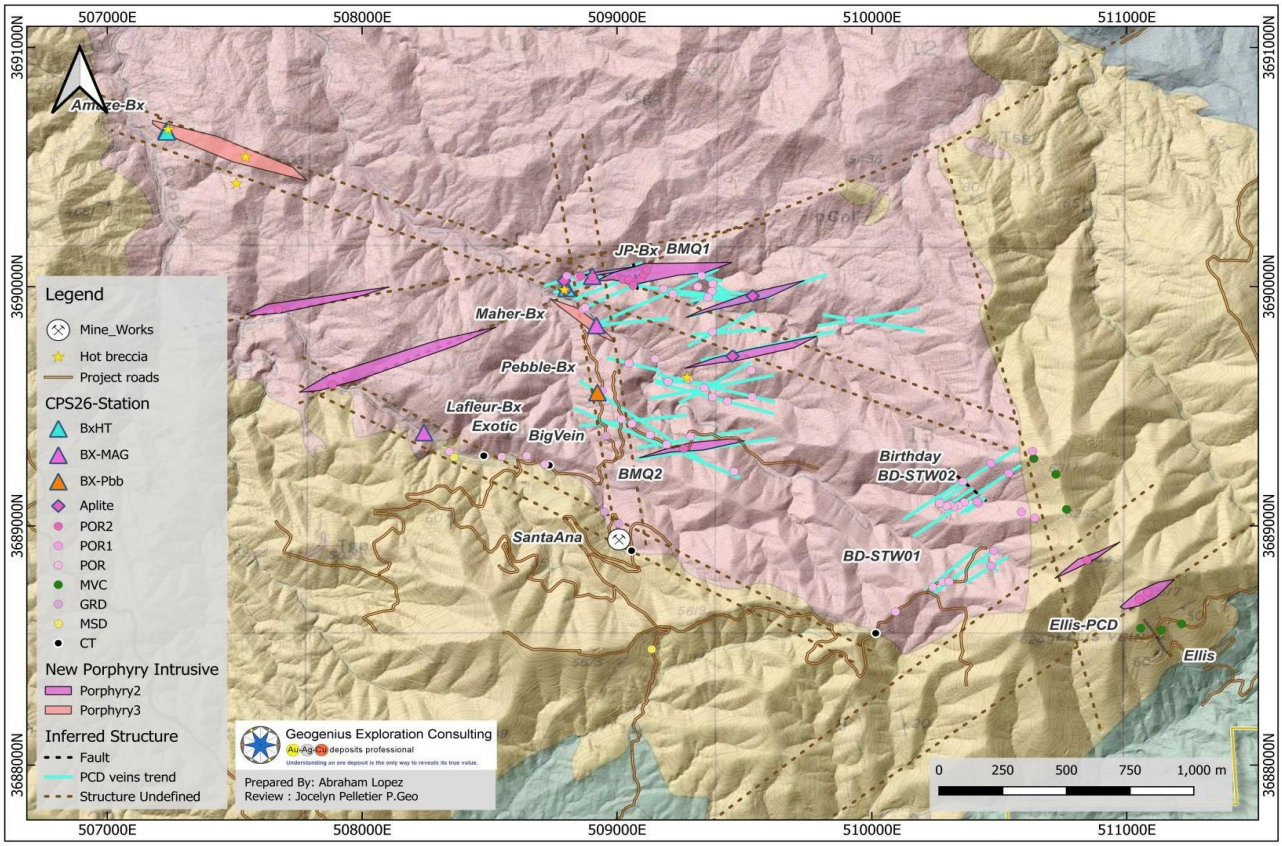


Figure 34: Draft Geology map of the recent work performed in spring 2026 on the Copper Spring Project. (1:15,000)

Joaquin area, an apical PCD architecture and its polyphased magmatic evolution

The Joaquin Area provides the most compelling evidence for emplacement within an apophysis portion of a Porphyry Cu-Mo Deposit (PCMD) characterized by geological features only find in such environment. Here are the principal geological evidences:

1. Glory Corridor: Structural corridor hosting a well-developed polyphased Cu-Mo Stockwork with potassic altered in a porphyric monzonite.
2. JP Breccia: Cu–Mo stockwork found in a multiphase porphyritic felsic intrusive magmatic breccia.
3. Maher breccia: Cu–Mo mineralisation within hydrothermal breccia found in strongly altered porphyric monzonite.
4. Mary Vein: Banded molybdenite–quartz (BMQ) in porphyric monzonite.

Glory-Corridor

The Glory Corridor host a well-developed polyphased Cu-Mo stockwork crosscutting from East to West with a vertical orientation in a Porphyric felsic intrusive. From surface expression, the corridor is more than 100m wide at more than 0.2%Cu, composed of multiple zones of 4-12m at +0.5%Cu where veinlets density reaches 8 to 20 veinlets per meter. This corridor shows a long lived strong structural control, recorded by local magmatic fabric, and brittle shear-oriented veinlets stock. The veins show a clear structural fabric, with typical

Shear and Reidel pattern on shear and veinlets suggesting a lateral component. The veinlets often overprint the same weakness pathway creating misleading aspect of the veins-composite.

The veins clearly show a distinct visual aspect, then common veins package found in PCMD, but veins mineralogy is similar. The veins show a clear pattern very easy to distinct one from the other, and here is a proposed sequence to recognise them:

- J-vein: Quartz-Feldspar veinlet with chalcopyrite ± bornite ± pyrite ± magnetite ± anhydrite, with strong pervasive halo of K-feldspar and white-mica. Pervasive style vein is 3-20mm wide, with alteration halo of 1-5cm, and 1-6% sulfides are in the vein disseminated to patchy and disseminated in the halo. Occasionally show 1mm center of pure chalcopyrite. Quartz is translucid, granular, gradual contact. Possibly Type-A vein.
- BMQ-vein: Banded molybdenite within quartz vein. Hard quartz vein is 3-30mm wide, with alteration halo of 1-2cm, and 2-25% banded molybdenite patches in only the vein. Quartz is translucid, granular, with sharp contact.
- K-vein: Quartz veinlet with Chalcopyrite ± pyrite ± molybdenite, with moderate alteration halo white-mica. Hard quartz vein is 3-50mm wide, with alteration halo of 1-3cm, and 1-15% sulfides are in the vein disseminated to patchy and disseminated in the halo. Quartz is granular with sharp contact. Possibly a variation of Type-B vein.
- BMQ-vein: Banded molybdenite within quartz vein. Hard quartz vein is 3-30mm wide, with alteration halo of 1-2cm, and 2-25% banded molybdenite patches in only the vein. Observed in Joaquin and Santa-Ana area. Quartz is translucid, granular, with sharp contact. Molybdenite is locally
- L-vein: Quartz veinlet with Chalcopyrite ± pyrite ± bornite ± molybdenite, with weak alteration halo white-mica. Quartz vein is 1-8cm wide, with alteration halo of less than 5mm, and 1-25% sulfides are only in the vein. Quartz is granular with sharp contact. Possibly a variation of Type-C vein.
- QSP-vein: Quartz veinlets with pyrite, with strong pervasive QSP alteration. Quartz vein is 1mm wide, with alteration halo of 1-8mm, and 1-5% disseminated pyrite in vein and halo. Quartz is dull, granular to glassy, with gradual contact. Possibly Type-D vein.
- PM-vein: Polymetallic quartz veinlets with pyrite ± sphalerite ± galena, with weak pervasive white-mica. Quartz vein is 3-30mm wide, with alteration halo of 1-10mm, and 1-3% disseminated to patches in only the vein. Quartz is dull, glassy, with sharp contact. Possibly Type-E vein.

CCMM veins show a similar paragenesis than the PCD, but they all have white-micas in their alteration halo, and this is probably due to muscovite content in the porphyry intrusive matrix.

Interpretation: Series of PCD veinlets channeled in a sub-vertical structural corridor crosscutting the PCD magmatic complex found in the Schultz intrusive complex. There is also commonly the presence of molybdenite combine to chalcopyrite in the K and L veins. Porphyry Cu-Mo deposit models suggest that high-concentration of molybdenite is found in the central part of porphyry copper deposits (Sillitoe, 2010, Cernuschi, 2026).



Figure 1: Stockwork with supergene malachite (green) in porphyric monzonite, Station CPS26-JP113.



Figure 2: Potassic alteration halo around quartz + sulfides veins, Easter zone, Station CPS26-JP101.



Figure 3: Magnetite-biotite alteration (Early Biotite vein?) in the monzonite, Joaquin, Station CPS25-JP029.

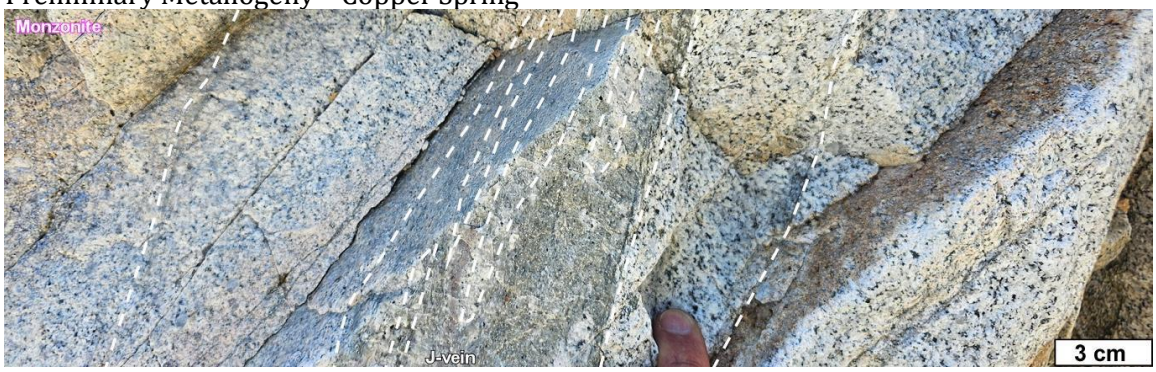


Figure 4: J-vein with multiple appendices showing fine chalcopyrite dissemination in a pervasive quartz-muscovite vein, in Porphyric Monzonite, Station CPS26-JP027.

Example of J-vein



Figure 5: J-vein showing pyrite-chalcopyrite dissemination in a pervasive quartz-muscovite vein, with Kspar alteration border of an altered Porphyric Monzonite, Station CPS26-JP073.



Figure 6: Type J-vein with strong pervasive quartz-mica, forming a gradual halo of chalcopyrite dissemination, on both side of the linear chalcopyrite center, Stockwow, Station CPS26-JP074.

Example of J-vein



Figure 7: Very wide J-vein with strong pervasive quartz-mica with forming a gradual halo of chalcopyrite dissemination in porphyry monzonite, BMQ2 zone, Station CPS26-JP107.



Figure 8: Very wide J-vein with strong pervasive quartz-mica with forming a gradual halo of chalcopyrite dissemination in porphyry monzonite, BMQ2 zone, Station CPS26-JP107.

Example of L-vein



Figure 9: L-vein compose of quartz showing 4% of chalcopyrite blebs, with very weak muscovite halo, Stockwow area, Station CPS26-JP073.

Example of K-vein

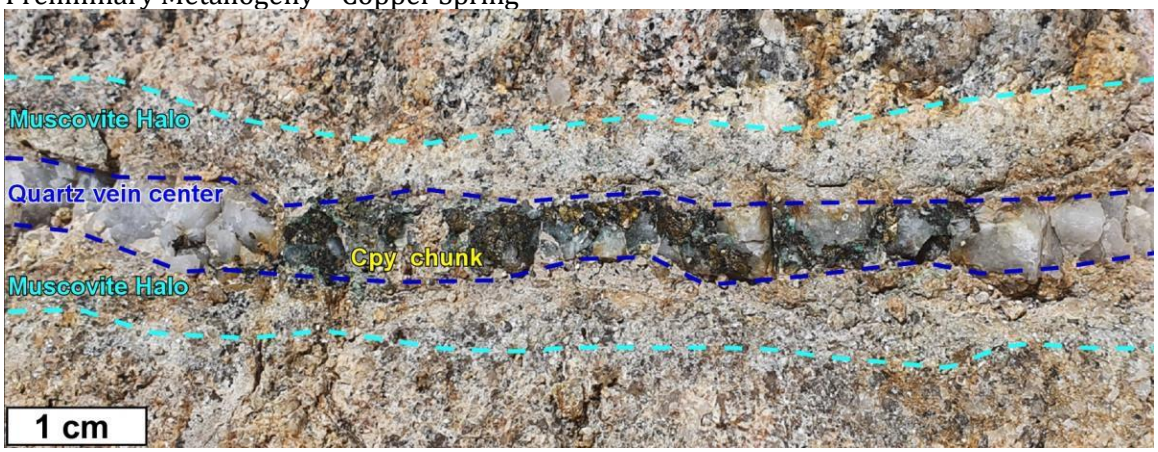


Figure 10: K-veins showing with pyrite-chalcopyrite cluster within a quartz center vein, surrounded by a moderate white-mica halo hosted in a Porphyric Monzonite, Joaquin area, Station CPS26-JP028.



Figure 11: K-veins showing with pyrite-chalcopyrite blebs within a quartz center vein, surrounded by a strong white-mica halo hosted in a Porphyric Monzonite, Joaquin area, Station CPS26-JP030. *Notice that the rock slab show a vertical view, were the veins forms an echelon and dip at 40m the South.*

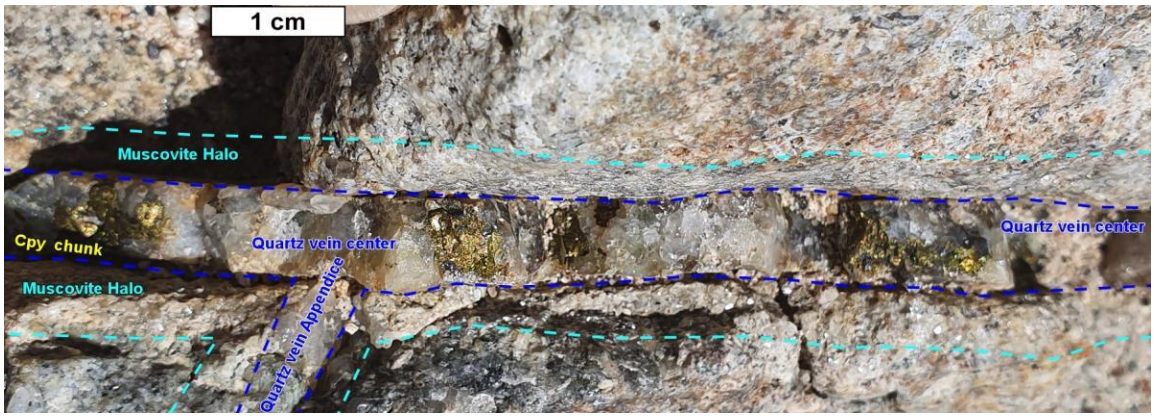


Figure 12: K-veins showing with chalcopyrite-pyrite blebs within a quartz center vein, with vein appendices, surrounded by a moderate white-mica halo, Joaquin area, Station CPS26-JP028.

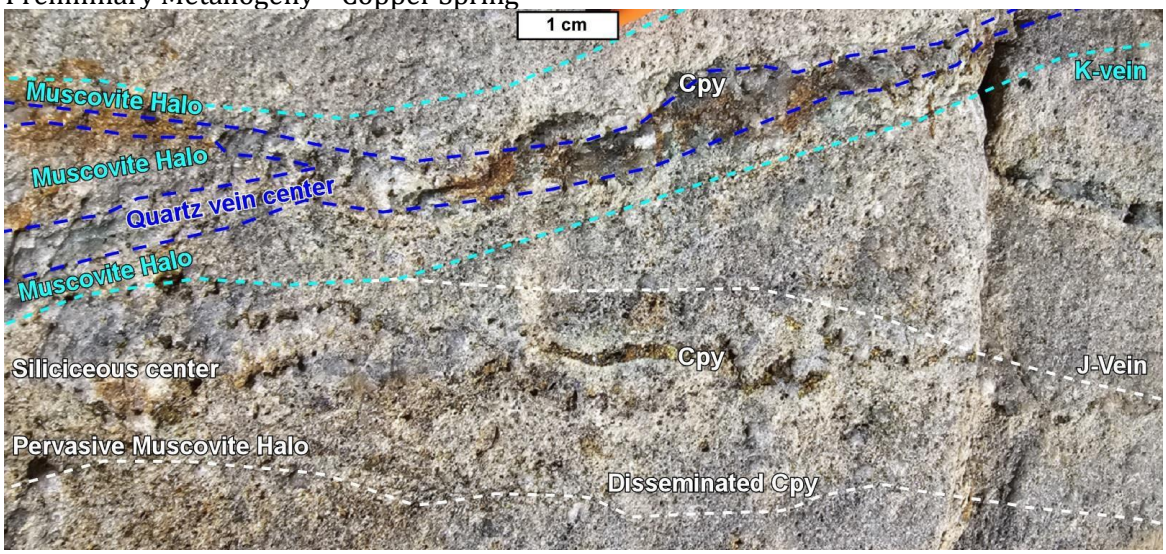


Figure 13: Type J-vein with strong pervasive quartz-mica with forming a gradual halo of chalcopyrite dissemination, crosscutted by K-vein with moderate white-mica halo. on both side of the linear chalcopyrite center, Stockwow, Station CPS26-JP074.

Example of BMQ-vein

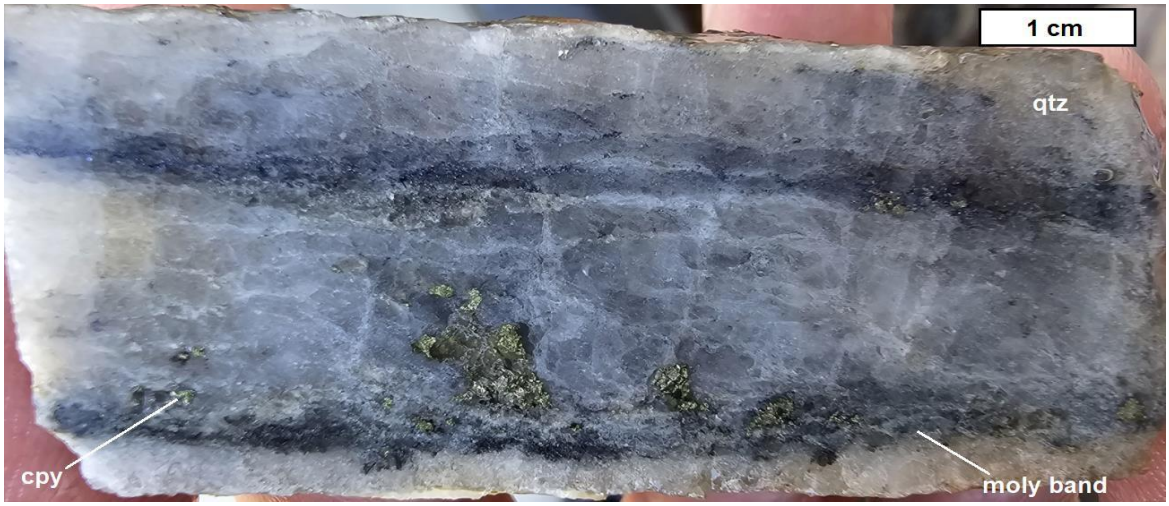


Figure 14: BMQ-vein with large molybdenite bands within a translucid quartz vein with patches of chalcopyrite, Joaquin Area, Station CPS26-JP038.



Figure 15: BMQ-vein with molybdenite bands within a translucid quartz vein with patches of chalcopyrite, BMQ2 Area, Station CPS26-JP107.

Example of D-vein



Figure 16: QSP-vein with bleaching sericitic halo surrounding a quartz vein with pyrite blebs, CS08-05 at 73.7m.



Figure 17: QSP-vein with bleaching sericitic halo surrounding a quartz vein with pyrite blebs, CS08-05 at 73.1m.



Figure 18: QSP-vein with bleaching sericitic halo surrounding a quartz vein with pyrite blebs, CS08-05 at 73.1m.

JP-Breccia

Found in the middle of this Joaquin area, the JP-breccia is a polyphase magmatic breccia intruding a porphyric monzonite intrusive hosting Cu-Mo stockwork. mineralisation. The Breccia was recognized by Jocelyn Pelletier, and documented for the first time in this report. At least four porphyritic intrusive phases are recognized in the JP magmatic breccia:

- Por1: leucocratic porphyritic monzogranite (10–15% biotite; 100–800 m scale), crosscut by
- Por2: melanocratic porphyritic monzonite (20–35% biotite–hornblende; 2–200 m wide), crosscut by
- Por3: mesocratic porphyritic monzonite (~20% biotite–hornblende; 2–10+ m wide), crosscut by
- Por4: late aplitic-like dykes with minor feldspar phenocrysts

These intrusive phases display clear crosscutting relationships, demonstrating repeated magmatic injections and sustained porphyric intrusive activity. This magmatic breccia is only exposed on 5m x 1m outcrop, but seems to forms a 20m x 2m zone. The JP-breccia is a brittle host-rock crosscutted by vertically oriented Cu-Mo mineralization, polyphased chalcopyrite–molybdenite veinlets stockwork of the Glory-Corridor.

Interpretation: This association of multiphase intrusive brecciation, vertical polyphase Cu–Mo stockwork, and late-stage molybdenite-bearing veining, are both diagnostic of the apical portion of a fertile magmatic apophysis, rather than a deep porphyry root zone.

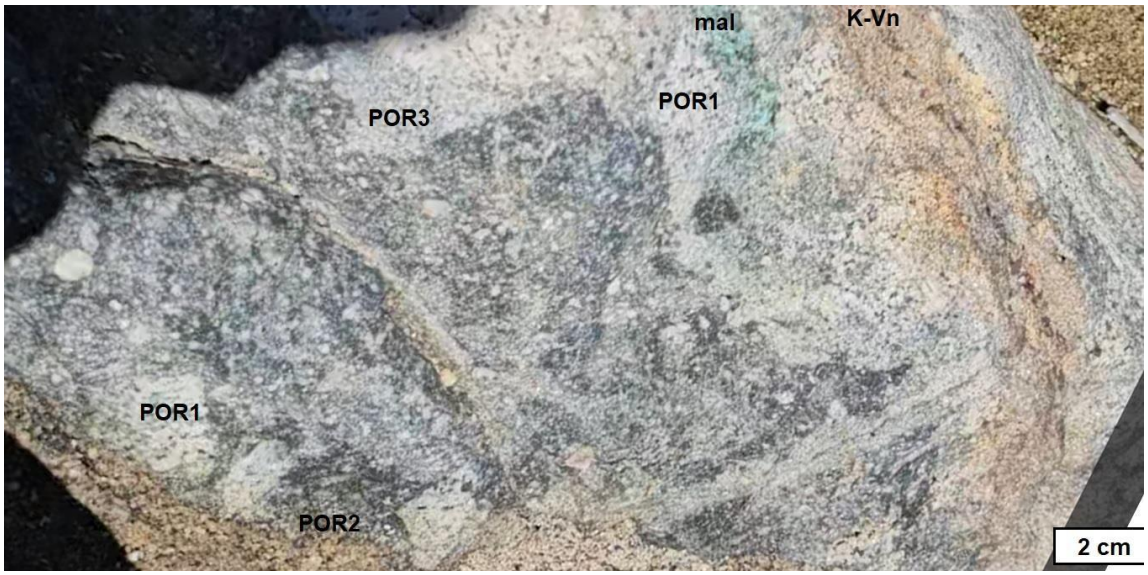


Figure 19: Fragments of Por1 intrusive in the POR2 intrusive, and fragments of POR2 in POR3 intrusive, all crosscutted by K-Vn vein, JP-Breccia, CPS25-JP027.

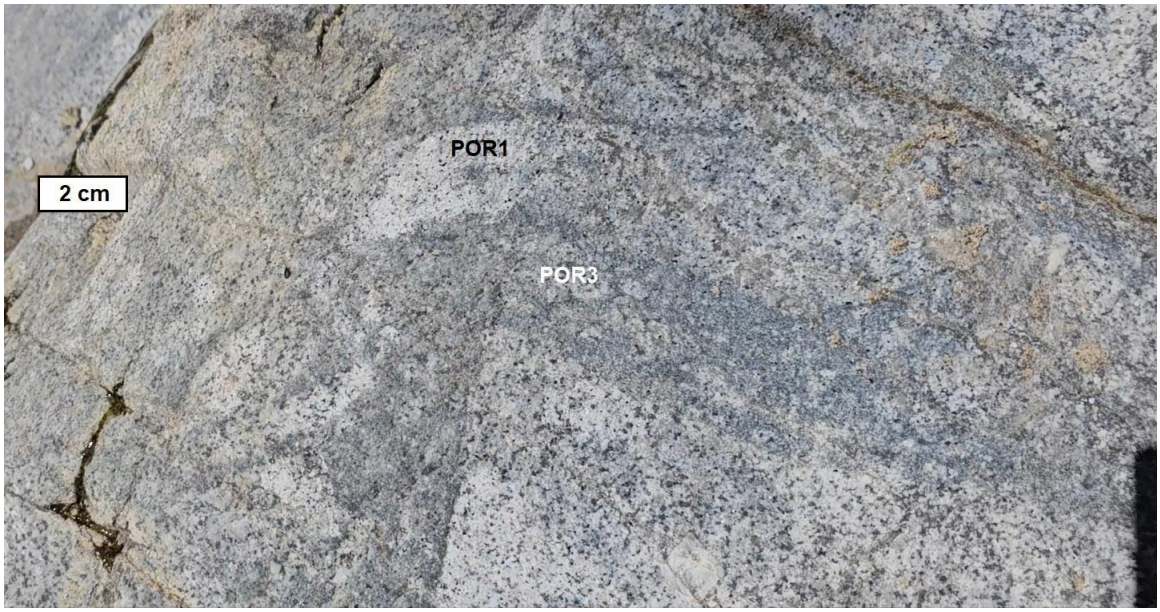


Figure 20: Magmatic breccia showing Fragments of Por3 intrusive within the POR1 intrusive (matrix), JP-Breccia, CPS25-JP027.

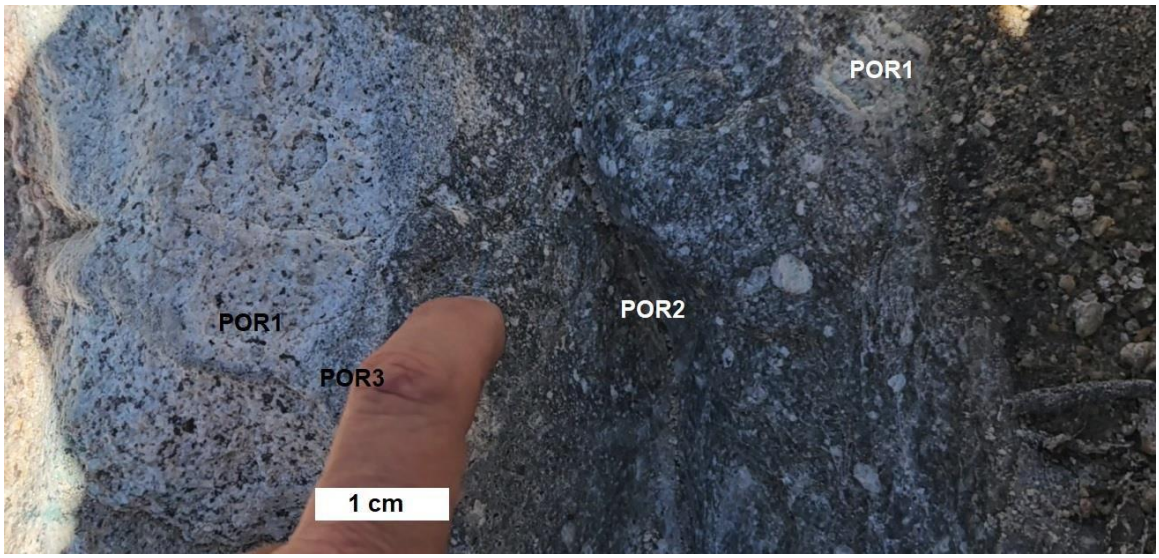


Figure 21: Fragments of Por1 in the POR2, and fragments of POR 2 in POR matrix2, CPS25-JP027.

Maher breccia

Hydrothermal breccia was recognized by David Maher in the Joaquin area., and its show typical quartz cement with local geodes with euhedral sulfides. The outcrop exposes a 10m x 4m hydrothermal breccia.

The fragments are angular to sub-angular composed of grey color muscovite rich metasomatized ''shist-like'' rock. The fragments came from a weakness zone in the porphyry intrusive where a decametric size metasediment xenolith was strongly metasomatized/replaced by a porous white-micas rich groundmass. The cement fills the space between the fragments with a whitish dull quartz with locally euhedral large quartz and euhedral patchy chalcopyrite-pyrite ± molybdenite. Aplitic dykes are found at proximity the Maher breccia., and are crosscutted by the cpy-mol veinlets stockwork of the Glory-Corridor.

This geometry indicates:

- focused fluid flow along chemically reactive and structurally prepared zones
- strong fluid–rock interaction
- hydraulic brecciation linked to magmatic fluid overpressure

Interpretation: Quartz-cemented hydrothermal breccias with Cu–Mo mineralization, spatially associated with intrusive phases and vertical stockwork development, are characteristic of the upper porphyry part to apical transition zone, where magmatic fluids are released and focused upward. This geological feature was observed at in Maria Mine part of the Cananea mine district, Sonora, Mexico.



Figure 22: General aspect of the hydrothermal breccia with white quartz cement, Maher-breccia, Station CPS26-JP026.

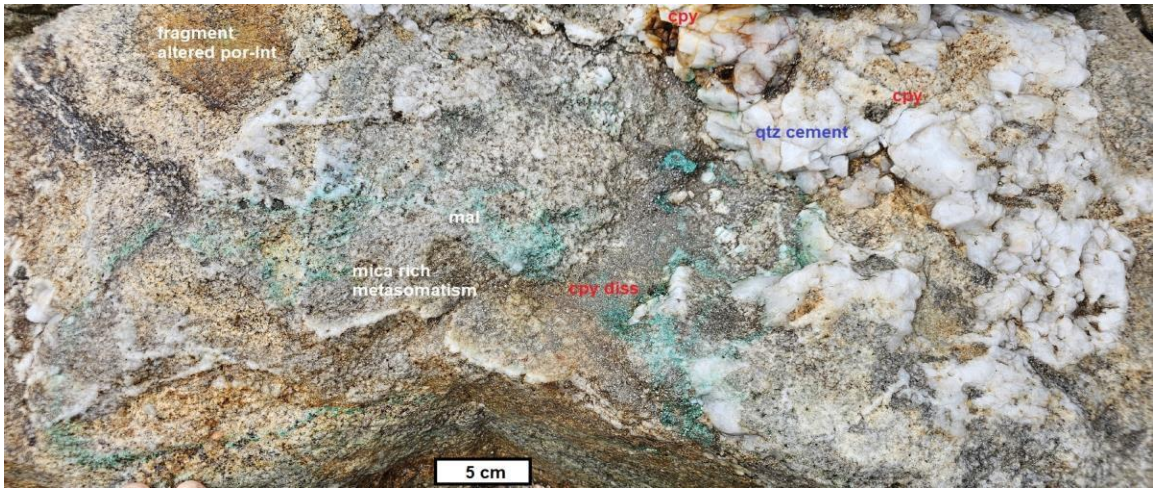


Figure 23: General aspect of the hydrothermal breccia with white quartz cement, Station CPS26-JP026.

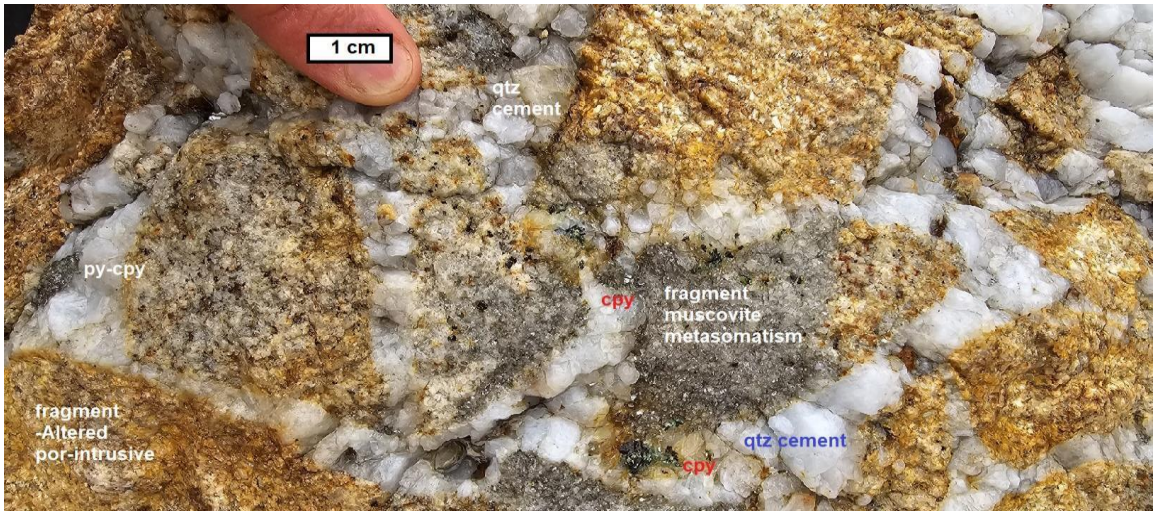


Figure 24: Close view of the hydrothermal breccia composed of altered porphyry-Intrusive and metasomatized muscovite rich altered fragments standing in the quartz cement with disseminated patched chalcopyrite-pyrite, Maher-breccia, Station CPS26-JP026.



Figure 25: Molybdenite- pyrite in quartz cement from hydrothermal breccia, Station CPS26-JP026.

Other Magmatic of Breccias

There are multiple additional magmatic breccias identified across the property, most of which form prominent topographic highs due to their higher quartz content within the matrix and/or the development of contact metamorphic–metasomatic alteration halos.



Figure 26: Magmatic breccia showing Fragments of Por2 intrusive within the POR1 intrusive (matrix), Lafleur-Breccia, CPS25-JP105.



Figure 27: Magmatic breccia with darker clasts porphyric intrusive (POR2) found in felsic leucocrate intrusive, all crosscutted by chalcopyrite bearing sheeted veins, BMQ2 zone, Station CPS25-JP107.



Figure 28: Magmatic breccia with darker fragments of metasediment found in felsic intrusive, Easter, Station CPS25-JP105.



Figure 29: Magmatic breccia with metric size fragments in porphyric intrusive, Station CPS-JP124.

Pebble breccia

Pebble breccias have also been identified on the property and are recognized as typical structural expressions developed in the upper and lateral portions of porphyry copper deposits (PCDs). The observed Pebble breccias are found next to the new phases of porphyric intrusive (POR2) composed predominantly of metasedimentary clasts derived from the Pinal Schist. The rounded morphology of the metawackes fragments indicates significant transport prior to breccia emplacement. Angular to subrounded fragments are found within pulverize fine grained matrix with the same composition of the fragment, testify the intensity of the explosive decompression.



Figure 30: Pebble breccia with monogenic composition, Easter, CPS26-JP106.

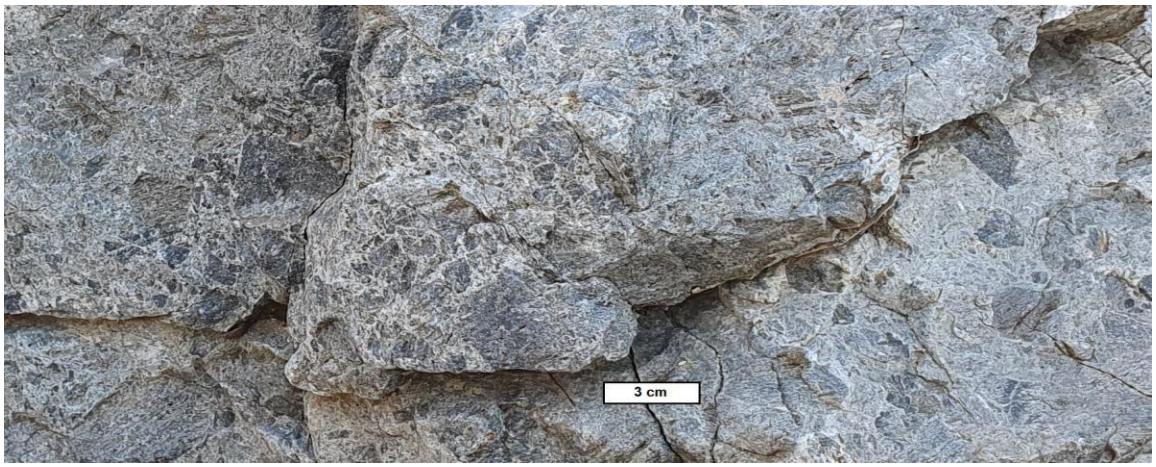


Figure 31: Angular to subrounded fragments of metawackes are found within pulverize fine grained matrix with the same composition of the fragment, Easter, CPS26-JP106.

Abundance of Molybdenite

BMQ veins were recognize in the Glory-Corridor and some of them have thickness size larger (10-30mm) than usual (3-10mm). The presence of a banded molybdenite–quartz (BMQ) vein is typically found in the central part of porphyry apophysis (Cernuschi, 2026). Unusual fact, there is also molybdenite combine to chalcopyrite in the K and L veins, suggesting anomalous concentration of molybdenite in the PCD type mineralisation. It is well-known that Molybdenite is found in the center part of the PCD deposit (Sillitoe, 2010, Halley, 2013, Cernuschi, 2026). At Glory-Corridor, the mol bearing veins are found at proximity of the Cpy rich veinlets, and both are found in a sericite altered porphyry rock.

Interpretation: Following the Halley metal zonation model, the Molybdenite veins are found in the apical portion of a fertile magmatic apophysis rather than a deep porphyry root zone.

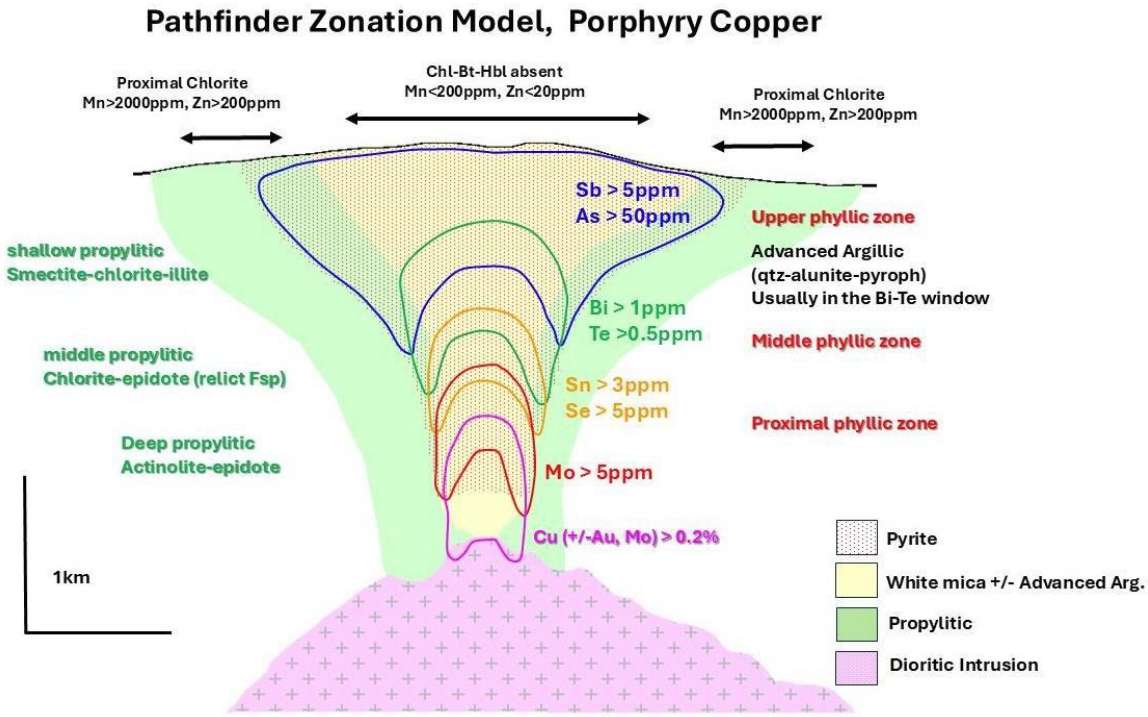


Figure 32: Schematic Alteration and Metal Zonation with a Porphyry Copper System (Halley, 2013).

District-scale vertical continuity of Cu–Mo stockwork and metasomatic footprint (Joaquin, Birthday, Santa-Ana, Ellis)

Across multiple zones on the Copper Spring Property, such Joaquin, Santa-Ana, Birthday, Ellis), a consistent and regionally coherent pattern is observed:

Joaquin Zone
- Porphyritic monzogranite cut by aplitic-like dykes
- Overprinted by vertical polyphased Cu–Mo stockwork
- Polyphased porphyric monzonite magmatic breccia (JP-Breccia)
- Cu-Mo hydrothermal breccia (Mayer Breccia)

Birthday Zone
- Porphyritic monzogranite cut by aplitic-like dykes
- Overprinted by vertical polyphased Cu–Mo stockwork
- Plurimetric Cu-oxides supergene coated zone

Ellis Mine
- Presence of porphyritic monzogranite with vertical Cu–Mo stockwork
- Copper mineralization related to quartz veinlets in propylitic-altered diorite

Santa Ana
- Vertical Cu–Mo veinlet-oriented stock crosscutting the Pinal Schist.
- Development of high-temperature QSP (greisen-like) mesothermal quartz vein
- Overprinting of Cu–Mo veinlet-oriented stock crosscutting the greisen zones
- Upward metasomatism propagation of magmatic fluids from a fertile source below

Lesage zone
- Porphyritic monzogranite cut by aplitic-like dykes
- Overprinted by vertical polyphased Cu stockwork
- Strong potassic alteration in stockwork

Hot-Breccias
- Hydrothermal breccia with quartz cement (Amaze-breccia)
- Magmatic breccia with porphyric qtz-monzonite intrusive

Interpretation: The recurrence of vertically oriented, polyphased chalcopyrite–molybdenite stockworks across multiple lithologies (intrusive and host rock), combined with high-temperature metasomatism and supergene expression, demonstrates:
- a vertically extensive and coherent hydrothermal system
- sustained magmatic fluid flux
- strong evidence for a fertile intrusive center at shallow to moderate depth

Discussion

Lithology

The Schultz Batholith (POR1) is a porphyritic felsic intrusive that assimilated significant amounts of felsic material from its host rocks, the Pinal metasediments. Depending on the degree of assimilation, the intrusive varies compositionally from monzonite to to qtz-diorite monzogranite. The batholith contains 5–15% euhedral porphyritic crystals, typically 1–5 cm in size, within a felsic matrix containing approximately 10–18% biotite.

A key unit that had never been properly mapped is a darker porphyritic monzonite intrusion (POR2), which crosscuts the Schultz Batholith (POR1). This porphyric intrusive range from Qtz-diorite to monzonite, and in particularly rich in biotite. When this intrusive show a darker color it is often due to the chloritisation of the biotite and amphibole. Most of the PCD-style stockwork mineralization is spatially associated with, or directly hosted by, this porphyritic intrusive phase.

A later felsic porphyry phase (POR3) is distinguished by its high concentration of feldspar and quartz phenocrysts within a coarse-grained felsic matrix. This porphyritic intrusive ranges compositionally from monzonite to monzogranite and is comparatively poorer in biotite. All hydrothermal breccias containing quartz-cemented matrices include fragments of this magmatic phase (POR3). This intrusive phase also appears spatially associated with mega-scale xenoliths of metasedimentary rocks enclosed within the Schultz Batholith.

All currently recognized PCD-style stockwork veinlets display white-mica alteration halos, interpreted as the result of high-temperature hydrothermal alteration producing abundant white mica and quartz around the veins. This alteration halo is most intensely developed within POR2 and POR3, although it is also present within the Schultz Batholith (POR1), suggesting elevated mica alteration within all porphyritic intrusive phases. Where the PCD veinlets are hosted by metasedimentary rocks, strong white-mica alteration halos are also well developed.

Halo from PCD veinlets are very distinct by there sericite with fine py-cpy disseminated mineralisation that the greisen metasomatism forming coarse crystals due to higher temperature assemblage of muscovite-quartz-pyrite (cubic).

Discussion

Upper part of the Porphyry Copper Deposit

Previous regional metallogeny model proposed that Copper Spring would be the lower part of Porphyry Copper System showing a poor potential. Recent observation describes in this report suggest that multiple outcrop exposed rocks corresponding of the upper part of a Porphyry Copper deposit:

- Porphyry dykes complex with parallel elongated porphyry felsic intrusives
- Specularite veinlets associate bleaching sericitic crackle breccia in Santa Ana
- Specularite-Chalcopyrite crackle breccia in Gibson mine
- The hydrothermal breccia with quartz cement of Mayer breccia
- The hydrothermal breccia fragment within the magmatic breccia of Easter breccia
- Molybdenite found in open-space of quartz veinlets in Santa Ana's drill core
- Banded quartz-feldspar veins in Santa Ana's drill core
- Cluster effect of the sulfides content within the K-vein and L-vein
- Pebble breccia

All these specific characteristics of Porphyry Copper System indicates that Copper spring is a structurally controlled Porphyry Copper Deposit. Deposits with similar features indicates clusters of apohysis aligned with specific structures, like Santo-Tomas (Sinaloa, Mexico), Yerington (Nevada, USA), Wafi-Golpu (Papua New Guinea), Filo del Sol (Argentina).

Conclusion

The combined observations made in its main mineralised zones; Joaquin, Birthday, Lesage, Ellis, and Santa Ana areas define a consistent geological framework characterized by:

- Multiphase intrusive magmatism and magmatic-brecciation
- Vertically oriented, polyphased Cu–Mo stockwork mineralization
- Cpy-Mol bearing hydrothermal brecciation with quartz cement
- Late-stage molybdenite-bearing quartz veining (BMQ)
- High-temperature metasomatism (greisen) country rocks

These features collectively support a position within the apical portion of a fertile porphyry Cu–Mo system, most likely at or near the top of a magmatic apophysis, rather than within a deeply eroded root zone.

The presence of unusual geological features, including sheeted veinlet stockwork mineralization and strong white-mica alteration halos surrounding PCD veinlets, contributed to uncertainty in the interpretations of previous geologists who evaluated the property. However, recent advances in the understanding of structurally controlled Porphyry Copper Deposits indicate that such features are common in several PCD systems (Perez-Florez, 2018; Pelletier, 2021; personal communication with David Cooke, 2025).

These new geological observations provide a completely renewed perspective on the potential for economic mineralization within the multiple PCD-style stockwork zones currently exposed over an area exceeding 3 km by 1 km.

Mr. Jocelyn (Josh) Pelletier, SEG-F, P.geo
QP Senior Geologist (OGQ # 961)
UQAM Msc Geology & Bsc Management
Canada: 001 (514) 913-7391
Mexico: 52 (1) 614 128-2576
Email: pgeo.jp@gmail.com
Au-Ag-Cu deposits Professional
Understand an ore deposit is the only way to reveal its true value.

COYOTE COPPER
MINES INC.
COPPER TRIANGLE - ARIZONA

Collaboration with

MineOro
EXPLORATIONS

References

Cernuschi, F., Dilles, J.H., Osorio, J., Proffett, J.M., & Kouzmanov, K. (2024). *Timing and temperature of copper and molybdenum precipitation in porphyry deposits*. Economic Geology, 119(5), 931–960.

Cernuschi, F.. (2026). *Timing and temperature of copper and molybdenum precipitation in porphyry deposits.* Eclectic rock, PDAC short sources session. March 2026.

Cooke, D.R., Hollings, P., & Walshe, J.L. (2014). *Giant porphyry deposits: Characteristics, distribution, and tectonic controls.* Economic Geology, 109(4), 877–889.

Guilbert, J.M., & Park, C.F. Jr. (1986). *The geology of ore deposits* (2nd ed., 985 pp.). New York: W.H. Freeman.

Halley, S., Dilles, J.H., & Tosdal, R.M. (2013). *Footprints: Hydrothermal alteration and geochemical dispersion around porphyry copper systems*. SEG Newsletter, 94, 1–17.

Hedenquist, J.W., Arribas, A., & Reynolds, T.J. (1998). *Evolution of an intrusion-centered hydrothermal system: Far Southeast-Lepanto porphyry and epithermal Cu–Au deposits, Philippines.* Economic Geology, 93(4), 373–404.

Lowell, J.D., & Guilbert, J.M. (1970). *Lateral and vertical alteration-mineralization zoning in porphyry ore deposits.* Economic Geology, 65(4), 373–408.

Monecke, T., et al. (2018). *Porphyry copper deposits: System evolution and controls on mineralization.* In J.W. Hedenquist et al. (Eds.), Economic Geology 100th Anniversary Volume (pp. 553–578). Society of Economic Geologists.

Tardani, D., Tassara, S., Sanchez-Alfaro, P., Reich, M., Pérez-Flóres, P., Robidoux, P., Contreras, C., Pinti, D. L., Cembrano, J., & Ague, J. J. (2024). *The orientation of intra-arc crustal fault systems influences the copper budget of magmatic-hydrothermal fluids.* Communications Earth & Environment, 5(1), Article 477. Springer Nature.

Piquer, J., Sanchez-Alfaro, P., Pérez-Flores, P. (2021). *A new model for the optimal structural context for giant porphyry copper deposit formation.* Geology, 49(5), 597–601. Geological Society of America.

Richards, J.P. (2011). *Magmatic to hydrothermal metal fluxes in convergent and collided margins.* Ore Geology Reviews, 40(1), 1–26.

Richards, J.P. (2015). *Tectono-magmatic controls on porphyry Cu-(Mo-Au) formation.* Economic Geology, 110(5), 1033–1056.

Seedorff, E., Dilles, J.H., Profett, J.M., Einaudi, M.T., Zurcher, L., Stavast, W.J.A., Johnson, D.A., & Barton, M.D. (2005). Porphyry deposits: Characteristics and origin of hypogene features. Economic Geology, 100(Special Issue), 251–298.

Sillitoe, R.H. (2010). Porphyry copper systems. Economic Geology, 105(1), 3–41.

Tosdal, R.M., & Richards, J.P. (2001) Magmatic and structural controls on the development of porphyry Cu ± Mo ± Au deposits. Reviews in Economic Geology, Vol. 14, pp. 157–181.